

# Impact of particle size reduction on glaze-melting behaviour

## Description by heating microscopy and Vogel–Fulcher–Tamman equation

Nataliia Gorodylova · Žaneta Dohnalová ·  
Petr Košťál · Petra Šulcová · Milan Vlček

Received: 27 September 2013 / Accepted: 15 November 2013 / Published online: 11 December 2013  
© Akadémiai Kiadó, Budapest, Hungary 2013

**Abstract** The effect of milling on thermal behaviour of two types of industrial ceramic glazes was investigated by heating microscopy. The Vogel–Fulcher–Tamman equation was used for viscosity calculation of the glaze samples, and the impact of particle size reduction on calculated data has been analysed. The employed model provides a good fit to the general tendencies of viscosity change during melting and can be applied for a comparative description of glaze-melting behaviour. Observed correlations between the viscosity, the contact angle, milling time, glazing temperature and the specular reflection of the glazed tiles help to reveal the optimal physical characteristics for glaze manufacturing and to achieve the desired gloss and smoothness of glazed surface. On its turn, variation of particle size distribution highly affects thermal behaviour of ceramic glazes, and thus, the milling procedure provides the possibility of manipulation of glaze-melting behaviour during heating and allows to change the manufacturing heating cycle when required.

**Keywords** Glaze-melting behaviour · Particle size distribution · Heating microscopy · Vogel–Fulcher–Tamman equation

### Introduction

The use of glaze on ceramic has an extensive history. The earliest glazed pottery appears to have been made in Iraq in the ninth century. From there, it spread to Egypt, Persia and Spain before reaching Italy in the Renaissance, Holland in the sixteenth century and other European countries shortly after. Glaze coating on ceramic is widely used nowadays, and the most frequently used material for these purposes is ceramic glaze. From a chemical point of view, ceramic glaze is a powdered glass substance which comprises a silicate network modified with alkalis and other elements to produce the desired properties. The main functions of glaze cover can be outlined as follows:

- to impart resistance to a body (strength, waterproofness, resistance to acids, etc.);
- to add hardness and environmental durability;
- to reduce exposed porosity (which improves cleanability and provides safety of foodware);
- to provide aesthetic qualities (colour, gloss, smoothness, etc.).

Physically, ceramic glaze is a thermodynamically unstable, intrinsically complex system, and its melting behaviour highly affects surface smoothness and homogeneity of glazed ware, bubble evolution, crystallisation and dissolution of pigments and fillers during firing [1, 2]. Therefore, understanding and describing melting behaviour of glazes are of great importance in the manufacturing of ceramic products. Considering the physical characteristics

---

N. Gorodylova (✉) · Ž. Dohnalová · P. Košťál · P. Šulcová  
Department of Inorganic Technology, Faculty of Chemical  
Technology, University of Pardubice, Doubravice 41, 532 10  
Pardubice, Czech Republic  
e-mail: nataliiaoleksandrivna.gorodylova@upce.cz;  
natasha.gorod@gmail.com

M. Vlček  
Institute of Macromolecular Chemistry, Academy of Sciences of  
the Czech Republic, Heyrovsky sq. 2, 120 06, Prague,  
Czech Republic

M. Vlček  
Joint Laboratory of Solid State Chemistry of Institute of  
Macromolecular Chemistry of the Academy of Sciences of the  
Czech Republic and the University of Pardubice,  
532 10 Pardubice, Czech Republic

of glazes, two of the most important parameters are viscosity ( $\eta$ ) and surface tension, which have the greatest impact on the glaze flow over the substrate, wettability and forming of a uniform glaze layer without draining of the surface as well as the facility of gas bubble elimination during glaze formation. In order to ensure a proper coverage and a smooth surface of ceramics, the glaze viscosity must be controlled, and at the peak firing temperature, its magnitude must pass in the range of  $10^3$ – $10^4$  Pa s [1, 2].

The viscosity magnitude, as well as mechanical behaviour of glaze systems, strongly depends on the temperature: below the glass transition temperature ( $T_g$ ), ceramic glaze behaves as an elastic solid and obeys Hooke's law; when at a high temperature, above complete melting ( $T_m$ ), it behaves as fluid, and the viscosity changes in almost perfect accordance with Arrhenius' law. However, technologically important withal complicated processes take place at the intermediate temperature range (between  $T_g$  and  $T_m$ ), where the glaze viscosity decreases progressively from the value of  $10^{12}$  Pa s down to  $10^2$  Pa s. As in the case of classical amorphous material, the viscous flow of glazes is thermally activated, and above the glass transition temperature, the activation energy is not constant. Theoretically, the best fit to viscosity data over  $T_g$ – $T_m$  range for ceramic glazes is provided by the Vogel–Fulcher–Tamman equation, which includes three variable constants. However, it is almost impossible to determine experimentally using direct measuring techniques. The main difficulties are connected with rapid increase of the molecular group mobility and devitrification danger when maintained at a constant temperature [2]. In addition, when using a common fast firing cycle ( $50\text{ }^\circ\text{C min}^{-1}$ ), the glaze system does not reach the equilibrium state due to faster temperature increase than required for heat transfer and melting processes; thus, the observed viscous flow at a constant temperature will not correspond to the complex viscosity changes during the fast heating cycle.

One of the most powerful research tools in comprehension of glaze behaviour in an actual industrial firing cycle is heating microscopy, which provides direct observation of a specimen and its shape changes [2]. The sample dimensions can be directly related to sintering, softening, flow, wetting of the substrate and surface tension as well as being used as indirect measurement of the viscosity during heating. Using the Vogel–Fulcher–Tamman equation, heating microscopy has been widely applied to describe the melting behaviour and viscosity calculations of different types of ceramic glazes [1–3] as well as for evaluation of pigment impact on the thermal processes during glazing [4]. However, in spite of great impact of particle size distribution of glazes on glaze-melting behaviour and surface appearance of glazed tiles [5–7], detailed in situ characterisation of particle size effect remains beyond the attention. Our investigation is devoted to the topic where we have employed hot stage microscopy and

the Vogel–Fulcher–Tamman equation for description of melting behaviour and viscosity calculations of glazes depending on particle size distributions. In addition, impact of particle size reduction on surface tension and surface appearance of glazed tiles have been analysed, and some correlations between particle size distribution, calculated viscosity data, surface tension, glazing temperature and surface appearance of enamel have been outlined for two ceramic glazes with a different composition.

### Theoretical part

Dependence of the viscosity of ceramic glaze on the temperature can be estimated indirectly using data provided by heating microscope and calculations based on the Vogel–Fulcher–Tamman equation (VFT):

$$\log \eta = A + \frac{B}{T - T_0}, \quad (1)$$

where  $A$ ,  $B$  and  $T_0$  are the unknown constants.

The calculations are based on the assumption that the viscosity of glazes at several characteristic points can be considered constant:  $\eta = 10^{12}$  Pa s at the glass transition point ( $T_g$ );  $\eta = 10^{10}$  Pa s at the beginning of sintering ( $T_s$ );  $\eta = 10^{3.55}$  Pa s at the half-sphere point ( $T_{1/2}$ ). Unknown parameters  $A$ ,  $B$  and  $T_0$  are determined by introducing three pairs of viscosity–temperature ( $\eta$ ,  $T$ ) values into a system of equations. As result, we obtain:

$$T_0 = \frac{12T_g - 3.55T_{1/2} + (9.25T_s - 12T_g) \times (T_{1/2} - T_g)/(T_s - T_g)}{8.45 - 2.75 \times (T_{1/2} - T_g)/(T_s - T_g)}, \quad (2)$$

$$A = \frac{9.25T_s - 12T_g + 2.75T_0}{T_s - T_g}, \quad (3)$$

$$B = (T_g - T_0) \times (12 - A). \quad (4)$$

By solving the system of equations, it is possible to calculate the value of the viscosity over the entire temperature range [2]. Graphically, the VFT equation can be represented with a straight line plot of  $\log \eta$  versus  $1/(T - T_0)$ , where  $A$  is the y-intercept,  $B$  is the slope of the line and  $T_0$  is the measure of deviation of the curve from the ideal straight line of nonassociated liquids. The above considered model is a general form which is possible to apply for different glaze compositions and firing conditions.

### Experimental

Two different types of commercial single firing transparent lead glazes (Glazura, CZ) with known composition were

**Table 1** Composition of the commercial ceramic glazes

Components/ mol%	SiO <sub>2</sub>	B <sub>2</sub> O <sub>3</sub>	Al <sub>2</sub> O <sub>3</sub>	PbO	CaO	Na <sub>2</sub> O	K <sub>2</sub> O
Type 1 G 050 91	51.4	13.8	8.6	12.5	9.5	1.4	2.8
Type 2 G 070 91	59.4	4.4	10	21.7	1.8	1.6	1.1

used in our experiments (Table 1). Milling of the samples was performed in acetone media with addition of a grinding filling (in mass ratio 1:10, type ZY, fraction 1.6–1.4  $\mu\text{m}$ , SiLyheads, Germany) using a laboratory planetary mill (Pulverisette 5, Fritsch, Germany; employed rotation speed 200 rpm) and agate milling forms during 5–60 min. The particle size distribution of the samples was measured using a laser scattering system based on Fraunhofer bending (Mastersizer 2000/MU, Malvern Instruments, UK). Scanning electron microscopy (SEM) was used to characterise the samples with respect to their particle size and homogeneity (JOEL JSM-5500 LV apparatus equipped with analyser IXRF Systems and detector Gresham Sirius 10, Joel Inc., USA). Differential thermal and thermogravimetric analysis (DTA/TG) was used for determination of the characteristic glass transition point of the glazes (Jupiter STA 449/C/6/F, Netzsch, Germany) with temperature intervals between 20 and 1,000  $^{\circ}\text{C}$ . The glass transition point was also determined with use of an optical dilatometer [TMA CX 03 (RMI, Czech Republic)]. The dilatometer measurement was performed with temperature intervals between 50 and 600  $^{\circ}\text{C}$  for glass samples with defined thermal history (cooling/heating rate 10  $^{\circ}\text{C min}^{-1}$ ). Softening and melting behaviour of the glazes placed on ceramic substrate was determined using a heating microscope (HM) with automatic image analysis (EM201-12, Hesse Instruments, Germany). The tests were performed with a constant heating rate of 50  $^{\circ}\text{C min}^{-1}$ , and a conventional industrial tile was chosen as a ceramic body. The equipment has been calibrated using Sn, In, Al, and Zn, and standard measurement uncertainty typically is  $\leq 5$   $^{\circ}\text{C}$ . For the measurement, pellets of cylindrical form with a diameter of 2 mm and with a height of 3 mm were prepared and placed into a specimen carriage in cylindrical tube furnace, where sample silhouette is analysed in the direct beam path during heating. The test of each sample was performed at least three times. Due to anomalous behaviour of the sample G 070 91—60 min, i.e. its strong interaction with air during heating which resulted in encapsulation of a substantial amount of air, the heating microscopy experiments of this sample were not reproducible, and these results are not included in the discussion. Gloss of enamelled tiles was measured using a glossmeter (ZGM 1110, Zehntner, Switzerland) with measurement geometry 20 $^{\circ}$  (high-gloss surfaces). The measurement of each sample was performed 10 times.

## Results and discussion

For our research, we have chosen two commercial lead glazes which are widely used in decorative pottery. Lead compounds play a very important role in glaze formation, and general characteristics of such glazes include low melting range (due to low melting point and the strong fluxing action of lead oxide), wide firing range, low surface tension, high index of refraction (responsible for brilliant gloss of lead glazes) and high resistance to devitrification. It also worth to mention that lead, being applied in a frit, where it is chemically combined in a glassy matrix and is kept tightly bonded, is not hazardous for usage and environment.

The particle size distribution of the glazes depending on the milling time was analysed using a laser scattering technique. Obtained results are presented as a size-bar diagram (Fig. 1), which represents characteristic diameter values— $d[10]$ ,  $d[50]$  and  $d[90]$ . The milling time highly affects the particle size and the distribution widths ( $\text{Span} = (d[90] - d[10])/d[50]$ ), which proportionally reduce with time increase. For example, for glaze G 050 91, span reduces from 3.63 to 1.76  $\mu\text{m}$  and for glaze G 070 91—from 3.66 to 2.14  $\mu\text{m}$ . The homogeneity of the glaze particles can also be followed from SEM images. Results for several samples with the corresponding particle size distribution on a logarithmical scale are presented in Fig. 2. From both data, it is easy to conclude that unmilled glazes have particles with two different size ranges, and an increase of the milling time lead to a decrease of the mean size values and improved homogeneity.

Calculation of viscosity data using VFT equation requires to determine the temperatures of three characteristic points: the glass transition point, the beginning of sintering and half-sphere point. The first point,  $T_g$ , corresponds to the transition from a disordered solid to a liquid and is characterised by a change in heat capacity and thermal expansion coefficient. Thus, two approaches can be used for its determination—DTA and expansion test using an optical dilatometer. We have employed both approaches, which provided well correlated results:  $T_g$  (G 050 91) = 550  $^{\circ}\text{C}$  and  $T_g$  (G 070 91) = 498  $^{\circ}\text{C}$ . On the DTA curve, the glass transition point appears as a step accompanied by a weak endothermic effect (Fig. 3). The step effect was observed clearly only for glaze G 050 91, which is presented in Fig. 3. Thermal expansion curves for both samples are presented in Fig. 4. On the curves, a change of the curve slope is observed at the glass transition point (Fig. 4), and this approach for determination of  $T_g$  point provides more precise and reliable result.

The beginning of sintering and half-sphere point of the glaze samples were determined using heating microscopy. The equipment provides direct observation of the specimen

**Fig. 1** Particle size distribution of the ceramic glazes depending on the milling time (0–60 min)

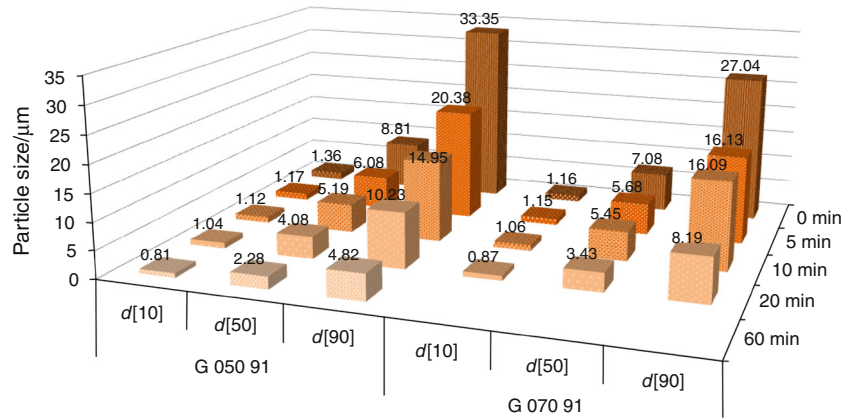


**Fig. 2** SEM images and particle size distribution of the ceramic glazes on a logarithmical scale

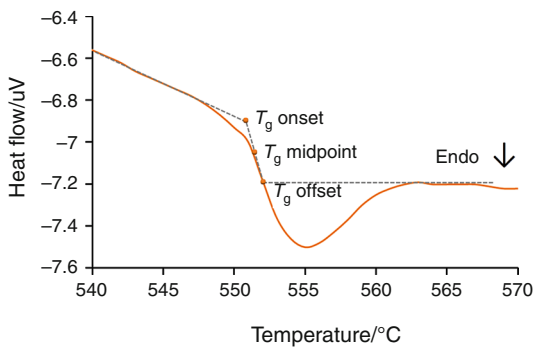
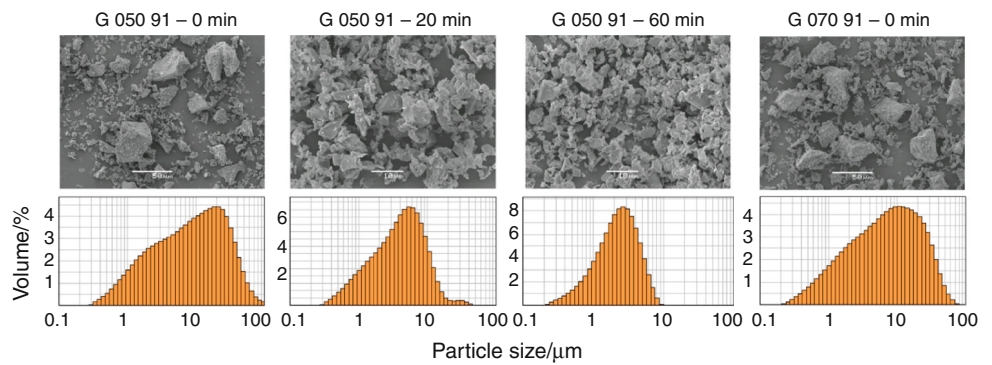


**Fig. 3** DTA curve of ceramic glaze G 050 91

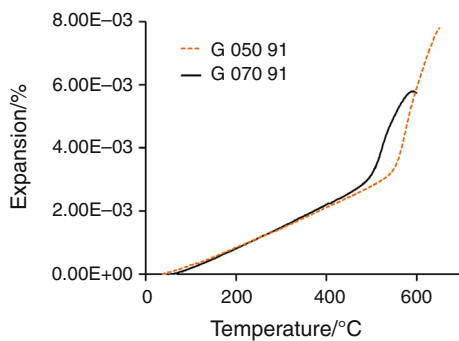


**Fig. 4** Results of expansion test of the samples

and the shape change during heating. To clarify the melting behaviour of ceramic glazes, Fig. 5 shows the initial height decrease of sample G 070 91 (not milled) with the characteristic shape points. The change of percentage of the initial height indicates the balance between gravitational, viscous and surface tension forces acting on the glaze during the melting process. The initial exponential decrease of its height corresponds to the sintering process, and the sintering beginning temperature ( $T_s$ ) is the point where the curve begins to slope. The deformation point ( $T_{def}$ ) corresponds to the first minimum, and the next expansion region on the curve refers to the sample deformation or rounding. From this point, the liquid phase prevails over the solid phase and emerges on the surface of the sample, which results in a sphere shape at higher temperature ( $T_{sph}$ ). The last important point is that of half-sphere ( $T_{1/2}$ ), which corresponds to the temperature at which the height of the sample is a half of its width and is used in calculation of the viscosity.

Equal tests were performed for two ceramic glazes with different particle size distribution; the data for sample G 050 91 depending on the milling time are presented in Fig. 6. The particle size decrease caused changes in melting behaviour of the samples, in particular glazes with lower mean size values began to sinter and deformed at lower temperatures (before the deformation point, the

**Fig. 5** Typical height change of ceramic glaze sample during heating with characteristic shape points

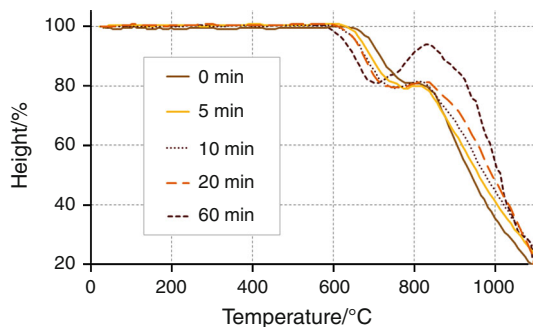
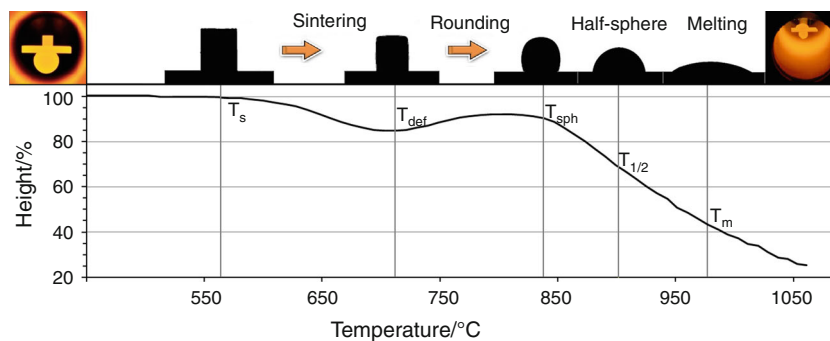


**Fig. 6** Height change of ceramic glaze G 050 91 during heating depending on the milling time (0–60 min)

curves drop under each other), while the sphere and the half-sphere points were reached at higher temperatures (the curves go on top of each other). For glaze G 070 91, the same tendencies, which shifted to lower temperatures, were observed. The effect observed at the low temperatures can be explained by a higher surface energy of the milled particles and, thus, higher driving force for grain growth and sintering to reduce the Gibbs energy of the system [8]. Furthermore, a higher amount of contact points between the particles activates the matter transport which leads to the high number of necks between particles, enhancing the diffusion with consequent densification and sintering [9]. The effect, which appears at the higher temperatures, in particular, deceleration of the melting processes, can be connected with a higher degree of association between little-sized particles, which may affect the viscous flow of the samples. Both effects are directly dependent on the milling time and the decrease of the particle size distribution.

A change of the contact angle during heating can be ascribed to interfacial tension between a melting glaze and a body surface. On Fig. 7, the data is presented for sample G 050 91, and the minimum on the plots corresponds to the highest interfacial tension, where the samples form a sphere shape. It can be well seen from the graphs that a decrease of the particle size leads to higher surface tension between the glaze and the ceramic body. Such effect of particle size reduction can be explained by greater affinity

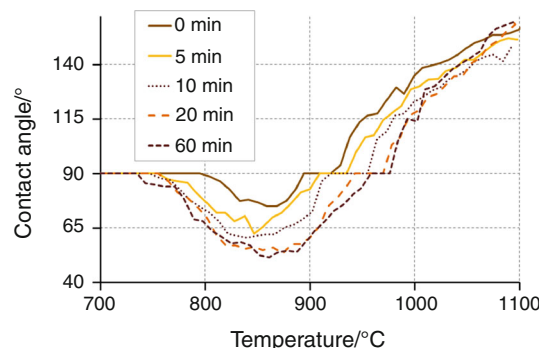


**Fig. 7** The variation of contact angle of ceramic glaze G 050 91 during heating depending on the milling time (0–60 min)

between the melted glaze and air which tends to increase the contact angle between the drop and the ceramic body. Similar behaviour was observed for glaze sample G 070 91, and described results are in good correspondence with those reported earlier [5, 7].

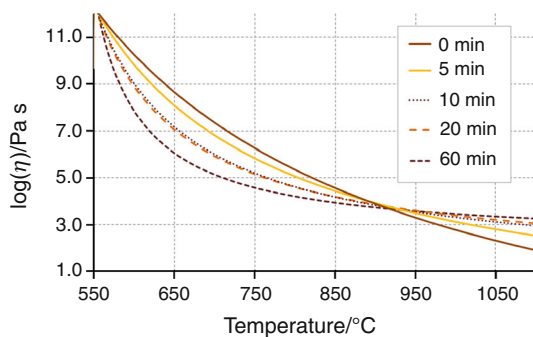
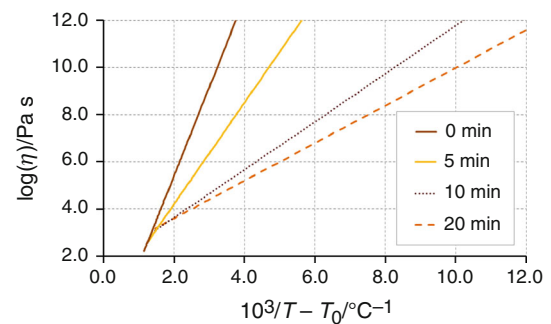
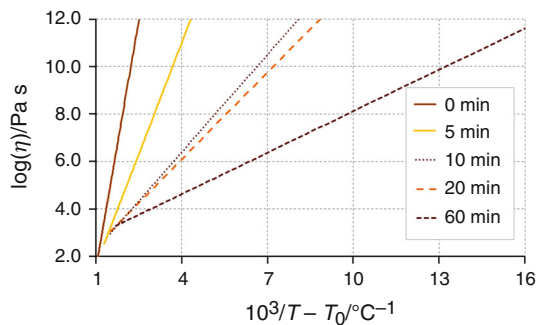
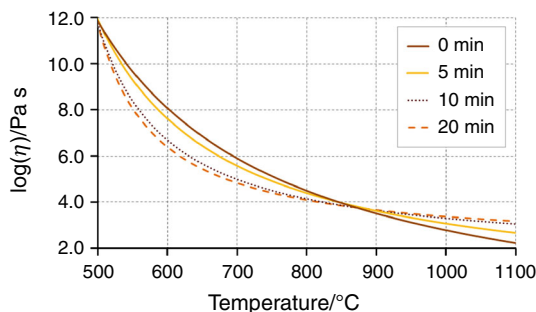
The glass transition ( $T_g$ ), the sintering beginning ( $T_s$ ) and the half-sphere temperatures ( $T_{1/2}$ ) were used to solve the system of the equations derived from the VFT Eqs. (2–4) and to calculate variation of the viscosity as a function of the temperature. The empirical reference temperatures of the glaze samples and the calculated coefficients of the VFT equation are summarised in Table 2. Obtained viscosity plots as logarithmical and linear slopes are presented in Figs. 8–11.

According to the calculations, it appears that the low-temperature effect observed by heating microscopy is also connected with a much quicker viscosity decrease of the milled samples. It makes sense taking into account the higher amount of contact points between milled particles which may also affect the viscous flow of the system. The opposite high-temperature effect has already been discussed above, and the calculated viscosity data supports our assumption concerning a higher degree of association between the little-sized particles at the high temperatures. However, the viscosity of the completely melted samples can't depend on the particle size of the initial ceramic glazes, and theoretically the viscosity curves must converge above the melting point of the glazes, where the VFT



**Table 2** Reference temperatures for the glaze samples and calculated coefficients of the VFT equation

Glaze	Milling time/min	$T_g/^\circ\text{C}$	$T_s/^\circ\text{C}$	$T_{\text{defl}}/^\circ\text{C}$	$T_{\text{sph}}/^\circ\text{C}$	$T_{1/2}/^\circ\text{C}$	$T_0/^\circ\text{C}$	$A$	$B$
G 050 91	0	555	629	805	859	925	157	-5.5	6,979
	5	555	614	765	864	940	324	-1.5	3,125
	10	555	596	757	885	955	431	0.9	1,373
	20	555	594	756	900	970	441	1.2	1,223
	60	555	579	743	905	977	495	2.3	582
G 070 91	0	498	563	706	842	901	231	-2.1	3,753
	5	498	550	695	848	905	321	-0.1	2,153
	10	498	533	690	858	917	400	1.6	1,017
	20	498	528	686	872	920	418	2.0	799

**Fig. 8** Variation of the viscosity as a function of the temperature: glaze G 050 91, 0–60 min of milling**Fig. 11** Straight line plots representing the VFT equation: glaze G 070 91, 0–20 min of milling**Fig. 9** Straight line plots representing the VFT equation: glaze G 050 91, 0–60 min of milling**Fig. 10** Variation of the viscosity as a function of the temperature: glaze G 070 91, 0–20 min of milling

model provides doubtful results. Another weak point of this approach is that the half-sphere point ( $T_{1/2}$ ) used for the calculation obviously is affected by the interaction of melted glaze with air (wetting angle and elimination of air bubbles), which impacts the sample height, which on its turn is affected by the particle size distribution. However, the VFT model provides a good fit to the general tendencies of the viscosity change during melting and can be applied only for a comparative description of glaze-melting behaviour.

An industrial property, which is related to the quality of the glazed surface, is their gloss, which can be determined in the ability of a surface to directly reflect light. It mostly depends on surface roughness and absorbance and can be measured by observing light reflection behaviour of surfaces using a glossmeter. The numerical values obtained from the measurement correspond to the surface reflection during light irradiation with a defined incidence angle. In our investigation, we have evaluated gloss of enamels which were glazed at three different temperatures: 950, 1,000 and 1,050 °C. Correlations between milling time (particle size distribution) of the investigated ceramic glazes, calculated viscosity data, glazing temperature and gloss of enamelled tiles can be observed in the diagrams presented in Figs. 12 and 13.

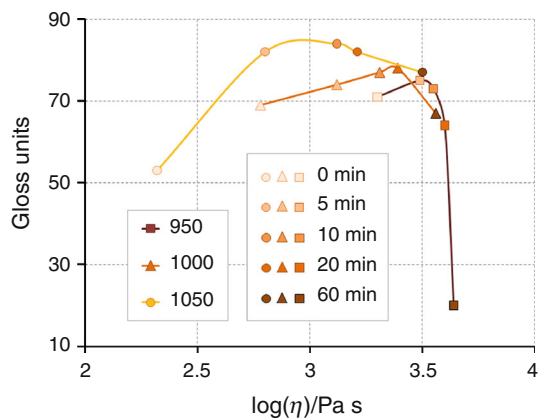


**Fig. 12** Correlations between gloss of enamelled tiles, glazing temperature, viscosity and milling time of ceramic glaze G 050 91

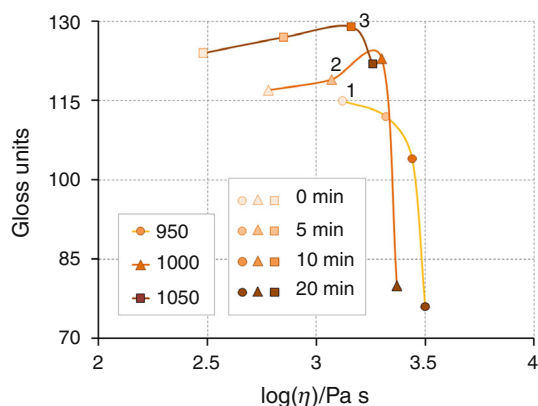


**Fig. 13** Correlations between gloss of enamelled tiles, glazing temperature, viscosity and milling time of ceramic glaze G 070 91

The dependences have an expected character, where some maxima are observed, which correspond to the highest gloss for each firing temperature and the optimal milling time for that type of glaze. In most cases, particle size reduction firstly provides a higher surface gloss, and its further decrease leads to a decrease of surface gloss too. When to analyse the curves more precisely, it can be easily concluded that the gloss is affected by viscous flow, but the surface tension has the same importance and surface appearance depends on the ratio between these two parameters. As example, we have analysed 3 points, which are shown in Fig. 13: point 1 corresponds to 0 min of milling time and a glazing temperature of 950 °C, point 2–5 min and 1,000 °C and point 3–10 min of milling and 1,050 °C. The glaze viscosity at these points can be assumed as a constant ( $\log \eta = 3.1 - 3.15$  Pa s), but if to analyse the contact angle, the unmilled sample at 950 °C has a higher surface tension than the milled samples at higher temperatures, which affects the surface appearance of the glazed tiles. Observed correlations between the viscosity, the contact angle, milling time, glazing

temperature and the specular reflection of the glazes during heating help to reveal the optimal physical characteristics and to achieve the desired gloss and smoothness of the glazed surface.

## Conclusions

The effect of milling on thermal behaviour of two types of industrial ceramic glazes was investigated by heating microscopy. The Vogel–Fulcher–Tamman equation was used for viscosity calculation of the glaze samples, and impact of particle size reduction on calculated data has been analysed. The effect of particle size reduction at the low temperatures consists of the decrease of sintering and deformation temperatures. It has been explained by a higher surface energy of the milled particles and, thus, a higher driving force for the grain growth and sintering to reduce the Gibbs energy of the system. In addition, a higher amount of contact points between the particles activates the matter transport, leading to a high number of necks between particles, which enhances the diffusion with consequent densification and sintering as well as affects the viscous flow of the glaze systems. An opposite effect appears at the higher temperatures, and observed deceleration of the melting processes can be connected with a higher degree of association between the little-sized particles and the calculated viscosity data supports our assumption. Thus, the VFT model provides a good fit to the general tendencies of the viscosity change during melting and can be applied for comparative description of glaze-melting behaviour. Observed correlations between the viscosity, the contact angle, milling time, glazing temperature and the specular reflection of the glazed tiles help to reveal the optimal physical characteristics for glaze manufacturing and to achieve the desired gloss and smoothness of glazed surface. In addition, variation of particle size distribution, which highly affects thermal behaviour of ceramic glazes, provides the possibility of the manipulation of glaze-melting behaviour and allows to change manufacturing heating cycle when required.

**Acknowledgements** The Ministry of Education, Youth and Sports of the Czech Republic, Project CZ.1.07/2.3.00/30.0021 ‘Enhancement of R&D Pools of Excellence at the University of Pardubice’, financially supported this work.

## References

1. Ahmed M, Earl DA. Characterizing of glaze-melting behaviour via HSM. *Am Ceram Soc Bull.* 2002;81:47–51.
2. Paganelli M, Sighinolfi D. Understanding the behaviour of glazes with the automatic heating microscope. *Proc Eng.* 2008;85:E63–7.
3. Boccaccini AR, Hamann B. Review in situ high-temperature optical microscopy. *J Mater Sci.* 1999;34:5419–36.

4. Salem Sh, Jazayeri SH, Bondioli F, Allahverdi A, Shirvani M. Characterizing thermal behavior of ceramic glaze containing nano-sized cobalt-aluminate pigment by hot stage microscopy. *Thermochim Acta*. 2011;521:191–6.
5. Bernardin AM. The influence of particle size distribution on the surface appearance of glazed tiles. *Dyes Pigment*. 2009;80:121–4.
6. Partyka J, Lis J. The influence of grain size distribution of raw materials on the selected surface properties of sanitary glazes. *Ceram Int*. 2011;37:1285–92.
7. Li J, Liang J, Wang L. Effect of particle-size distribution on the surface appearance of glazed surface. *J Therm Anal Calorim*. 2013. doi:[10.1007/s10973-013-3397-4](https://doi.org/10.1007/s10973-013-3397-4).
8. Jiang Q, Zhang SH, Li JC. Grain size-dependent diffusion activation energy in nanomaterials. *Solid State Commun*. 2004;130:581–4.
9. Santos C, Koizumi MH, Daguano JKMF, Santos FA, Elias CN, Ramos AS. Properties of Y-TZP/Al<sub>2</sub>O<sub>3</sub> ceramic nanocomposites obtained by high-energy ball milling. *Mater Sci Eng A*. 2009;502:6–12.